



Swansea University
Prifysgol Abertawe



Cronfa - Swansea University Open Access Repository

This is an author produced version of a paper published in:

AIP Advances

Cronfa URL for this paper:

<http://cronfa.swan.ac.uk/Record/cronfa51527>

Paper:

Way, A., Luke, J., Evans, A., Li, Z., Kim, J., Durrant, J., Hin Lee, H. & Tsoi, W. (2019). Fluorine doped tin oxide as an alternative of indium tin oxide for bottom electrode of semi-transparent organic photovoltaic devices. *AIP Advances*, 9 (8), 085220

<http://dx.doi.org/10.1063/1.5104333>

This item is brought to you by Swansea University. Any person downloading material is agreeing to abide by the terms of the repository licence. Copies of full text items may be used or reproduced in any format or medium, without prior permission for personal research or study, educational or non-commercial purposes only. The copyright for any work remains with the original author unless otherwise specified. The full-text must not be sold in any format or medium without the formal permission of the copyright holder.

Permission for multiple reproductions should be obtained from the original author.




Authors are personally responsible for adhering to copyright and publisher restrictions when uploading content to the repository.

<http://www.swansea.ac.uk/library/researchsupport/ris-support/>

Fluorine doped tin oxide as an alternative of indium tin oxide for bottom electrode of semi-transparent organic photovoltaic devices

Cite as: AIP Advances 9, 085220 (2019); <https://doi.org/10.1063/1.5104333>

Submitted: 26 April 2019 . Accepted: 13 August 2019 . Published Online: 21 August 2019

Amirah Way, Joel Luke , Alex D. Evans, Zhe Li, Ji-Seon Kim , James R. Durrant, Harrison Ka Hin Lee, and Wing C. Tsoi 



View Online



Export Citation



CrossMark

AVS Quantum Science

Co-published with AIP Publishing



Coming Soon!

Fluorine doped tin oxide as an alternative of indium tin oxide for bottom electrode of semi-transparent organic photovoltaic devices

Cite as: AIP Advances 9, 085220 (2019); doi: 10.1063/1.5104333

Submitted: 26 April 2019 • Accepted: 13 August 2019 •

Published Online: 21 August 2019



Amirah Way,¹ Joel Luke,²  Alex D. Evans,³ Zhe Li,⁴ Ji-Seon Kim,²  James R. Durrant,^{1,5} Harrison Ka Hin Lee,^{1,a)} and Wing C. Tsoi^{1,a)} 

AFFILIATIONS

¹SPECIFIC, College of Engineering, Swansea University, SA1 8EN Swansea, United Kingdom

²Department of Physics, Imperial College London, SW7 2AZ London, United Kingdom

³School of Physics and Astronomy, Cardiff University, Cardiff CF24 3AA, United Kingdom

⁴School of Engineering, Cardiff University, CF24 3AA Cardiff, United Kingdom

⁵Department of Chemistry and Centre for Plastic Electronics, Imperial College London, SW7 2AZ London, United Kingdom

^{a)}Electronic mail: K.H.Lee@Swansea.ac.uk and W.C.Tsoi@Swansea.ac.uk

ABSTRACT

Indium tin oxide (ITO) is commonly used as the transparent bottom electrode for organic solar cells. However, it is known that the cost of the ITO is quite high due to the indium element, and in some studies ITO coated glass substrate is found to be the most expensive component of device fabrication. Moreover, indium migration from ITO can cause stability issues in organic solar cells. Nevertheless, the use of ITO as the bottom electrode is still dominating in the field. Here, we explore the possibility of using fluorine doped tin oxide (FTO) as an alternative to ITO for the bottom electrode of organic solar cells particularly on semi-transparent cells. We present side-by-side comparisons on their optical, morphological and device properties and suggest that FTO could be more suitable than ITO as the bottom electrode for glass substrate based organic photovoltaic devices.

© 2019 Author(s). All article content, except where otherwise noted, is licensed under a Creative Commons Attribution (CC BY) license (<http://creativecommons.org/licenses/by/4.0/>). <https://doi.org/10.1063/1.5104333>

A transparent electrode is essential for solar cells as it allows incoming light to reach the photoactive layer. Transparent conductive oxides (TCO) such as indium tin oxide (ITO) and fluorine doped tin oxide (FTO) are well-suited for this purpose due to their transparent and conductive nature. In the organic solar cell (OSC) community ITO is far more popular than FTO as the transparent bottom electrode. However the price of indium, which usually has a fraction of more than 70% in the ITO, is relatively high compared to fluorine and tin, and depends on global supply and demand.¹ Studies revealed that the cost of the ITO coated substrate is the highest among the material costs (including active layer, interlayers, top electrode and encapsulation) for manufacturing organic photovoltaic modules.^{2,3} Besides the cost, indium from the ITO was found to diffuse into the layers on top and even to the top metal electrode in normal device structure which may lead to

instability of devices.^{4,5} This scenario was also observed in organic light emitting diodes (OLED) which employ similar materials and device architecture.^{6,7} Nevertheless, ITO is still widely used in the field of OSC.

A few studies tried to use FTO to replace ITO as the bottom electrode for both OSC and OLED.^{8,9} For OSC, FTO was found to outperform the ITO, in terms of the high temperature processability and stability.⁸ FTO was found to have higher thermal stability than ITO. Sima et al. showed that the sheet resistance of ITO can go up from 18 Ω/\square to 52 Ω/\square after thermal annealing at 450 °C, while FTO remains unchanged.¹⁰ If interlayers which require high annealing temperature like titanium dioxide are employed, FTO is more suitable than ITO.^{11,12} Besides, FTO with lower sheet resistance (7-8 Ω/\square) is more mature than ITO and they are widely available in the market.¹³ Practically, lower sheet resistance is found

to have higher scalability of the device fabrication.¹⁴ Lucera et al. showed that OSC modules using FTO with a resistance of $8 \Omega/\square$ has a higher fill factor (FF) when compared to OSC modules using ITO with a resistance of $20 \Omega/\square$.¹⁵ On the other hand, for OLEDs, better performance was shown when using FTO when compared to ITO within the tested bias range.⁹ Furthermore, FTO coated glass is highly favourable for window glazing and can have low emissivity for thermal insulation.^{16–18} Therefore, it could be attractive to study the performance of semi-transparent OSC fabricated on FTO coated glass. However, quite often, the devices fabricated on FTO suffer from high leakage current due to the high surface roughness.

Here, we compare ITO and FTO as the bottom electrode for OSCs and explore the suitability of using FTO for OSCs, with particular interest in semi-transparent OSCs. Inverted poly[4,8-bis(5-(2-ethylhexyl)thiophen-2-yl)benzo[1,2-b; 4,5-b']dithiophene-2,6-diyl-alt-(4-(2-ethylhexyl)-3-fluorothieno[3,4-b]thiophene-)-2-carboxylate-2-6-diyl]:[6,6]-phenyl- C_{71} -butyric acid methyl ester (PTB7-Th:PC₇₁BM) was selected as a benchmark OSC system for this study.¹⁹ Their surface morphologies, optical properties and device characteristics were investigated. Through all-round comparison, we discuss and conclude how suitable FTO is as a bottom contact for OSC.

Patterned ITO and FTO substrates were purchased from Shanghai B.Tree Tech Consult Co. and Kintec Co. (NSG Pilkington FTO glass TEC15) respectively. The size and pattern of the substrates were the same, as were the sheet resistances, $15 \Omega/\square$. The substrates were sequentially cleaned by sonication in detergent, DI water, acetone and isopropanol in an ultrasonic bath. The substrates were then treated with oxygen plasma for 2.5 minutes right before spin-coating the first layer.

Inverted PTB7-Th:PC₇₁BM (purchased from 1-Material and Solenne BV, respectively) devices were fabricated for this study with ZnO as electron transport layer and MoO₃ as hole transport layer. Zinc oxide precursor solution (0.219 g zinc acetate dihydrate + 60.4 μ l ethanalamine + 2 ml 2-methoxyethanol) was spin-coated onto oxygen plasma cleaned substrates at 4000 rpm for 40 s followed by thermal annealing on a 150 °C hotplate for 10 minutes in air, resulting in a thickness of ~ 30 nm. The samples were then transferred to a nitrogen filled glovebox for active layer deposition. PTB7-Th and PC₇₁BM with 1:1.5 weight ratio were dissolved in chlorobenzene at 60 °C for at least 12 hours before spin-coating. 1,8-diiodooctane (3 vol%) was added to the solution 30 minutes before the deposition resulting in a total concentration of 25 mg/ml. The PTB7-Th:PC₇₁BM solution was spin-coated onto the ZnO layer at 900 rpm for 60 s, resulting in a thickness of ~ 100 nm. Films thicknesses were measured by a profilometer (Alpha-Step D-600 Stylus Profiler). The films were then transferred to an evaporator for MoO₃ (10 nm) and Ag (100 nm for opaque devices and 20 nm for semi-transparent devices) evaporations. Thickness calibrations of MoO₃ and Ag were done prior to the evaporations with the aid of the profilometer. The device area is 0.15 cm^2 . All opaque devices were encapsulated with UV-epoxy (Solarmer) before exposing to air.

Current density-voltage ($J-V$) characterisation was performed using a sourcemeter (Keithley 2400) under a solar simulator with an intensity of 100 mW/cm^2 . EQE spectra were obtained using a quantum efficiency measurement system (PV Measurements QEX10).

Where relevant a black background was used when testing the semi-transparent cells.

The UV-Vis transmission spectra of ITO, FTO and the semi-transparent cells were measured with a Perkin Elmer Lambda 750 spectrophotometer.

Non-contact Atomic force microscopy (AFM) measurements were taken using a Park NX10 AFM system and SmartScan software with Park silicon PPP-NCHR tips (force constant 42 N/m) with a resonant frequency of 300 - 330 Hz and a set point of approximately 10 nm. At least three regions on each sample were imaged to ensure reliability. Images were corrected for background to improve the image quality using the Gwyddion open-source software package.

AFM was employed to study the surface morphology of different layers on ITO and FTO, the AFM height images are shown in Figure 1a–1f. Firstly, we looked at the surface roughness of the ITO and FTO. As expected, the surface of FTO was much rougher than that of ITO, root mean square roughness (R_{rms}) of 0.63 nm for ITO and 16.0 nm for FTO. Furthermore, on the FTO surface (Figure 1d), there are tall features, tens of nanometres taller than the average. We then probed the surface roughness layer-by-layer up to the bulk-heterojunction (BHJ) active layer. After depositing the ZnO layer onto the TCO, the R_{rms} of the ITO/ZnO surface increases slightly to 1.7 nm whilst the R_{rms} of the FTO/ZnO surface drops by almost half, to 8.96 nm. After depositing the BHJ layer onto the ZnO, the R_{rms} of the ITO/ZnO/BHJ surface remains similar, 1.43 nm whilst the R_{rms} of FTO/ZnO/BHJ surface decreases further to 3.59 nm. Figure 1g summarises the sequential changes in surface roughness. It clearly shows that after ZnO and active layer deposition on the FTO substrate the surface roughness is substantially reduced, with the both layers on the two TCOs showing a more comparable surface roughness. Additionally, the distinct peaks observed on the FTO surface were absent in the ZnO and active layer images.

Next, we studied the device performance based on the device architecture shown on Figure 1h using either ITO or FTO as the bottom electrode. Figure 2a shows the $J-V$ characteristics of representative scans of the devices under one sun illumination and the corresponding device parameters are listed in Table I. The $J-V$ curves show comparable device performance for all parameters for both the TCO devices. These results are further confirmed by a statistical study on more than 10 devices for each TCO. Both the TCOs show comparable average and best power conversion efficiency (PCE) as shown in Figure 2b. Even though the short circuit currents (J_{SC}) are similar the spectral responses of each device are different. External quantum efficiency (EQE) of the devices are plotted in Figure 2c. Both spectra show a range from ~ 300 nm to ~ 850 nm mainly determined by the active layer absorption. However, the high-energy onset of the EQE spectrum for the FTO device is slightly shifted toward longer wavelengths which is directly correlated to the onset of the transmittance between the ITO and the FTO glass substrates (see the inset in Figure 2c). The difference in transmittance also causes some variation in the EQE spectra of the devices at other wavelengths. However, these variations are not significant and the calculated short-circuit current density (J_{cal}) from the EQE spectra of the ITO and FTO devices showing similar values of 14.87 mA/cm^2 and 14.63 mA/cm^2 , respectively. These values are in good agreement with the J_{SC} obtained under one sun, with a variation of $\sim 10\%$.

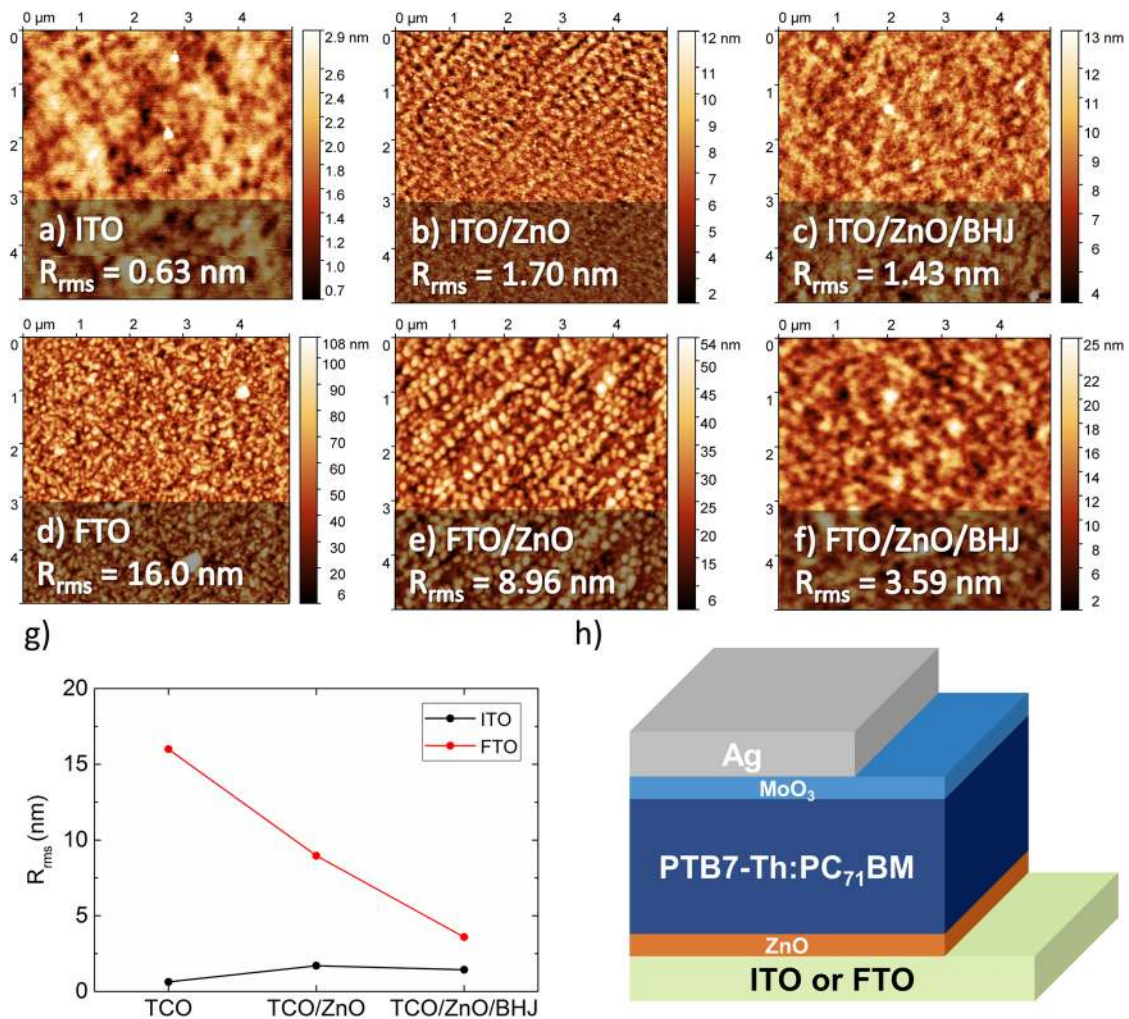


FIG. 1. AFM images and root mean square roughness (R_{rms}) of (a) ITO, (b) ITO/ZnO, (c) ITO/ZnO/BHJ, (d) FTO, (e) FTO/ZnO and (f) FTO/ZnO/BHJ. (g) R_{rms} obtained from the AFM images of the different surfaces. (h) Device architecture of the OSC in this study.

Energetically ITO and FTO have different work functions, -4.7 eV for ITO and -4.4 eV for FTO are the most common values reported in the literature.^{20,21} This difference in contact energy levels may affect open-circuit voltage (V_{OC}) in the devices.^{22,23} However, there is no difference in the V_{OC} for the devices studied here. This is probably due to the ZnO layer applied on top of the TCOs, which modifies the energy levels of the electrodes, resulting in similar energy level alignment. It is worth noting that the thickness of the ZnO is only about 30 nm which appears to be substantial to planarise the rough FTO surface, as seen in the AFM images.

Both ITO and FTO devices show comparable FF of ca. 64%. Series resistances (R_S) and shunt resistances (R_{Sh}) are extracted from the J - V curves. Since the sheet resistance of both the TCOs were purposely kept the same ($15 \Omega/\square$) as well as using identical TCO pattern, interlayer, active layer and top metal electrode, it is expected

that the R_S of both devices are similar. Although the sheet resistance can be kept the same, the roughness of the ITO and FTO are quite different. Usually, FTO is much rougher than ITO and it may cause higher leakage current in the devices.⁸ Importantly, here, both the R_{Sh} and the dark current density of the ITO and FTO devices are comparable as shown in Table I and Figure 2d, respectively. These results are consistent with the significant reduction in the roughness on the FTO substrate after coating the layers on top.

Furthermore, we deposited a thin silver layer (20 nm) to replace the opaque electrode in order to study the effect of the roughness of the top surface of the active layer (using ITO and FTO bottom electrodes, respectively) to the performance of semi-transparent OSC. The results are also shown in Figure 3 and Table I. Overall the performance decreased when compared to that of the opaque devices due to loss in J_{SC} as the whole devices are semi-transparent and

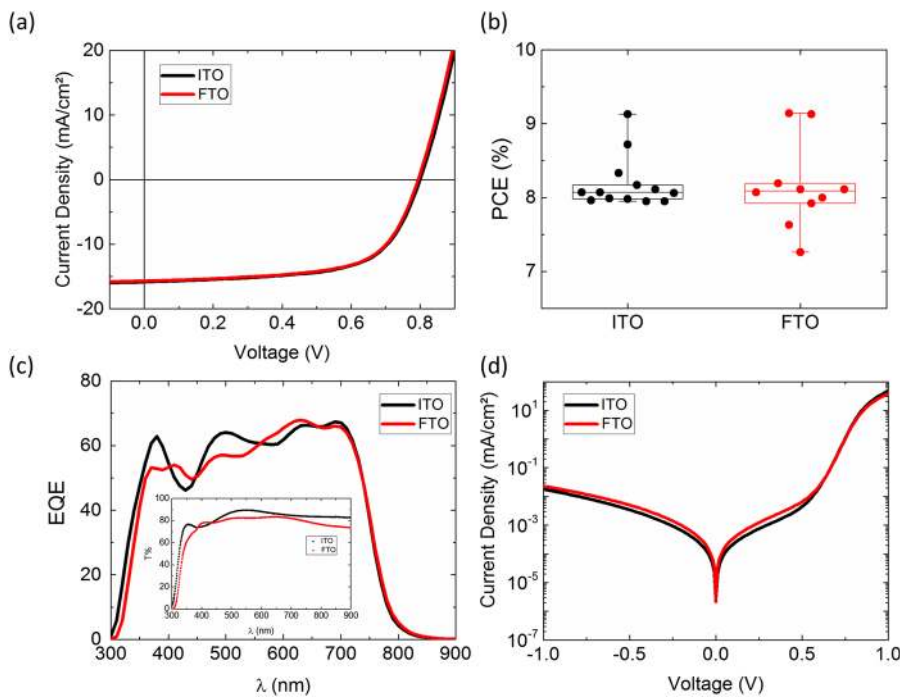


FIG. 2. (a) J - V characteristic of representative PTB7-Th:PC₇₁BM devices using ITO and FTO as the bottom electrode under one sun condition, (b) Statistical data of the PCE shown in box plots where the horizontal lines within the box indicate the medians, boundaries of the box indicate the 25th and 75th percentiles, whiskers indicate the minimum and maximum values of the results, and the data points are shown as dots, (c) EQE spectra of the devices and the inset of the transmittance of ITO and FTO glass substrates, (d) dark current density of the representative devices.

reflection by the back electrode is much reduced. Although the J_{SC} and V_{OC} of these semi-transparent devices are similar, the FF of the FTO device is slightly lower than the ITO device which is likely due to the slightly higher R_S of the FTO devices which can be attributed to the reduced conductivity of the thin silver layer on a rougher surface. This result suggests that the higher surface roughness of the active layer using FTO as bottom electrode has only minimal effect on the device performance, with overall performance being very similar. On top of that, the devices on FTO has slightly higher transmission in the visible region (Figure 3b). It is worth noting that the effect of the rough FTO surface could be further reduced with a thicker active layer which is more common in using up-scaling coating methods, hence the performance of semi-transparent OSC fabricated on FTO substrates could be even closer to that on ITO substrates.

OSCs with a device architecture of TCO/ZnO/BHJ/MoO₃/Ag fabricated on ITO and FTO with identical device configuration are

studied and compared. Their performance, series resistance, shunt resistance and dark current density are all comparable. Through probing the layer-by-layer surface roughness by AFM, the comparable results are well explained by the evolution of the surface roughness of the layers. The ZnO planarises the rough FTO surface resulting in the roughness reduced by almost half, from R_{rms} of 16 nm to a R_{rms} of less than 9 nm. The BHJ layer (PTB7-Th:PC₇₁BM) further planarises the surface and results in the R_{rms} to 3.59 nm which is more comparable to the roughness of the active layer using the ITO as bottom electrode (1.43 nm). Furthermore, the semi-transparent devices with a thin layer of silver as the top electrode further confirm that the rougher FTO surface is not a real concern after deposition of the subsequent layers. Therefore, FTO could be attractive to serve as the bottom electrode of OSC, especially semi-transparent OSC as FTO are useful for window glazing. Although ITO possesses some unique advantages over FTO, such as smoother surface and compatibility with flexible substrates, FTO can still be attractive given

TABLE I. Device parameters of the ITO and FTO devices. Opaque and semi-transparent device data are average values with the standard derivation (SD) from at least 10 individual devices and 5 individual devices, respectively. R_{Sh} and R_S are extracted from the inverses of the slopes at J_{SC} and V_{OC} , respectively. All devices have the same device area of 0.15 cm².

Device type	J_{SC} (mA/cm ²) Average ± SD	V_{OC} (V) Average ± SD	FF (%) Average ± SD	PCE (%) Average ± SD	R_{Sh} (Ω cm ²) Average ± SD	R_S (Ω cm ²) Average ± SD
ITO (opaque)	16.13 ± 0.73	0.79 ± 0.01	64.04 ± 1.03	8.19 ± 0.35	678.55 ± 97.76	5.58 ± 0.83
FTO (opaque)	16.08 ± 0.90	0.80 ± 0.01	63.46 ± 2.91	8.16 ± 0.59	651.83 ± 62.46	5.59 ± 0.68
ITO (20 nm Ag)	11.80 ± 0.22	0.79 ± 0.01	59.45 ± 2.86	5.54 ± 0.30	701.45 ± 149.39	12.53 ± 2.76
FTO (20 nm Ag)	11.57 ± 0.31	0.79 ± 0.01	57.13 ± 1.34	5.23 ± 0.16	680.39 ± 35.40	14.13 ± 3.89

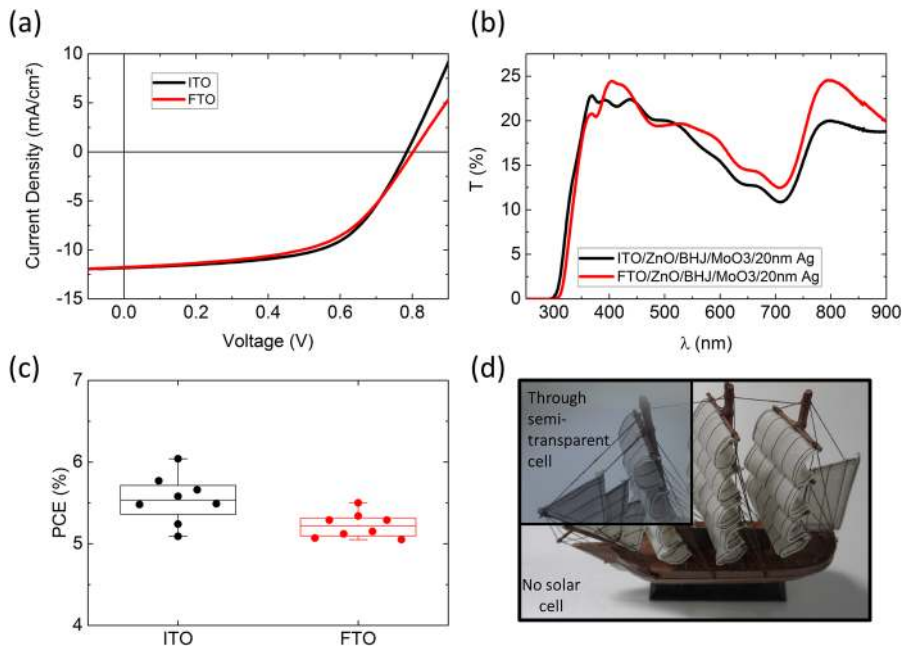


FIG. 3. (a) J - V characteristic of representative semi-transparent PTB7-Th:PC₇₁BM devices using ITO and FTO as the bottom electrode under one sun condition, (b) Transmittance of semi-transparent PTB7-Th:PC₇₁BM devices using ITO and FTO as the bottom electrode substrates, (c) Statistical data of the PCE, (d) Image through a semi-transparent PTB7-Th:PC₇₁BM device.

the similar device performance achieved herein, lower material cost, higher tolerance to the processing temperature and lower sheet resistance coating ready in the market. Flexible solar cells are also not essential for many applications such as solar cells integrated into windows for buildings and greenhouses. For these scenarios, making solar cells on rigid glass substrates, with FTO is perhaps more suitable.

The authors would like to acknowledge NSG Pilkington, the M2A funding from the European Social Fund through the Welsh Government. We are grateful to the Ser Cymru funding from the Welsh Assembly Government (Ser Solar), the SPECIFIC Innovation and Knowledge Centre (EP/N020863/1) funding, and the UK EPSRC for the Plastic Electronics Centre for Doctoral Training (EP/L016702/1) funding. Z.L. thanks the Welsh Assembly Government Ser Cymru II fellowship scheme for financial support.

REFERENCES

- M. Lokanc, R. Eggert, M. Redlinger, M. Lokanc, and R. Eggert, "The Availability of Indium: The Present, Medium Term, and Long Term" (2015).
- B. Azzopardi, C. J. M. Emmott, A. Urbina, F. C. Krebs, J. Mutale, and J. Nelson, *Energy Environ. Sci.* **4**, 3741 (2011).
- C. J. M. Emmott, A. Urbina, and J. Nelson, *Sol. Energy Mater. Sol. Cells* **97**, 14 (2012).
- M. Jørgensen, K. Norrman, and F. C. Krebs, *Sol. Energy Mater. Sol. Cells* **92**, 686 (2008).
- P. Cheng and X. Zhan, *Chem. Soc. Rev.* **45**, 2544 (2016).
- A. R. Schlatmann, D. W. Floet, A. Hilberer, F. Garten, P. J. M. Smulders, T. M. Klapwijk, and G. Hadziioannou, *Appl. Phys. Lett.* **69**, 1764 (1996).
- M. P. De Jong, L. J. Van Ijzendoorn, and M. J. A. De Voigt, *Appl. Phys. Lett.* **77**, 2255 (2000).
- W. H. Baek, M. Choi, T. S. Yoon, H. H. Lee, and Y. S. Kim, *Appl. Phys. Lett.* **96**, 1 (2010).
- A. Andersson, N. Johansson, P. Broms, N. Yu, D. Lupo, and W. R. Salaneck, *Adv. Mater.* **10**, 859 (1998).
- C. Sima, C. Grigoriu, and S. Antohe, *Thin Solid Films* **519**, 595 (2010).
- G. K. Mor, K. Shankar, M. Paulose, O. K. Varghese, and C. A. Grimes, *Appl. Phys. Lett.* **91**, 152111 (2007).
- R. Steim, F. R. Kogler, and C. J. Brabec, *J. Mater. Chem.* **20**, 2499 (2010).
- <https://www.pilkington.com/en/global/products/product-categories/special-applications/nsg-tec-for-technical-applications>, 2019.
- P. Meredith and A. Armin, *Nat. Commun.* **9**, 5261 (2018).
- L. Lucera, F. Machui, P. Kubis, H. D. Schmidt, J. Adams, S. Strohm, T. Ahmad, K. Forberich, H. J. Egelhaaf, and C. J. Brabec, *Energy Environ. Sci.* **9**, 89 (2016).
- D. S. Bhachu, M. R. Waugh, K. Zeissler, W. R. Branford, and I. P. Parkin, *Chem. A Eur. J.* **17**, 11613 (2011).
- N. Noor and I. P. Parkin, *J. Mater. Chem. C* **1**, 984 (2013).
- A. Anderson, S. Chen, L. Romero, and R. Binions, *Buildings* **6**, 37 (2016).
- Z. He, B. Xiao, F. Liu, H. Wu, Y. Yang, S. Xiao, C. Wang, T. P. Russell, and Y. Cao, *Nat. Photonics* **9**, 174 (2015).
- N. Balasubramanian, *J. Electrochem. Soc.* **138**, 322 (2006).
- Q. Qiao and J. T. McLeskey, *Appl. Phys. Lett.* **86**, 153501 (2005).
- N. K. Elumalai and A. Uddin, *Energy Environ. Sci.* **9**, 391 (2016).
- Q. Qiao, J. Beck, R. Lumpkin, J. Pretko, and J. T. McLeskey, *Sol. Energy Mater. Sol. Cells* **90**, 1034 (2006).